

## Imperfect pitchfork bifurcation with weak noise and an application to superfluid turbulence in liquid helium

Mark F. Schumaker and Werner Horsthemke

*Ilya Prigogine Center for Studies in Statistical Mechanics, Department of Physics,  
The University of Texas at Austin, Austin, Texas 78712-9990*

(Received 27 January 1987)

In this paper we analyze a model containing the unfolded normal form of the imperfect pitchfork bifurcation with additional terms representing additive white noise and a linear Ornstein-Uhlenbeck noise. After linearizing the model about a branch of stable steady states, we investigate the variance of fluctuations about these steady states as a function of a control parameter. We apply our model to experimental data obtained by Griswold, Lorensen, and Tough [Phys. Rev. B 35, 3149 (1987)] on the transition between superfluid turbulent states T-I and T-II in liquid-helium counterflow experiments. Our model accounts qualitatively for the steady states, relaxation times, and the variance of fluctuations which were measured in this system. Furthermore, our model predicts the existence of a curve of unstable steady states which have not yet been observed. Perturbations from the known steady state in the direction of these new unstable steady states are expected to lead to qualitatively new dynamics.

### I. INTRODUCTION

Nonlinear physical and chemical systems can show a rich variety of steady and dynamical behavior. We can gain some understanding of the underlying physical mechanisms by studying instabilities in these systems and transitions between their various states. Generally it is only for the simplest nonlinear systems that a complete theoretical description is available. However, if the nature of an instability or transition can be identified, it is often possible to develop a model of the system which describes its dynamical features at least over a certain region in parameter space and which can lead to further physical insight by predicting additional phenomena. The correct identification of the nature of an instability in the system would obviously be facilitated by a catalog of the transitions that can occur in a dynamical system and some measure of their likelihood. This is the subject of bifurcation theory.

Bifurcation theory attempts to describe all of the ways in which dynamical systems can make transitions from one state of motion to another. It has become a very powerful phenomenological tool for analyzing changes of states in physical systems. When transitions are made between steady states a very complete description of the different possibilities is given by singularity theory.<sup>1</sup> These different possible transitions are categorized according to a notion of complexity, the "codimension" of the bifurcation. The codimension counts essentially the number of external parameters which have to be equal to a particular numerical value for the bifurcation to occur. Bifurcations of low codimension are expected to be the most common in typical systems, because fewer conditions need be met. Singularity theory provides archetypical examples of equations containing each bifurcation, called "normal forms" of the bifurcation. These are, in a

sense, the simplest possible equations which contain the bifurcation. The steady states of a general model can be related to those of the normal form via a smooth local transformation about the singular point. Thus if we can properly identify the underlying bifurcation for an instability of a physical system, then the normal form provides a satisfactory model of the system, at least in the vicinity of the instability. This approach has been very successful in complex nonlinear chemical reactions, where generally the reaction mechanism is only incompletely known. It has led to a better understanding of experimentally observed phenomena and advanced our understanding of the dynamical behavior of nonequilibrium chemical reactions.<sup>2</sup>

There are various methods available in nonlinear dynamics, based on time series analysis, phase-space reconstruction, Poincaré sections, etc., that help with the identification of the underlying bifurcation. Here we will discuss yet another method based on an analysis of the fluctuations of the system in the vicinity of the bifurcation point. All macroscopic systems are subject to small irregular influences that cannot be modeled in a set of deterministic equations. We shall call these influences "noise." These may be "internal fluctuations," due to the complex interaction of the parts of a composite system, or they may be "external noise," due to an irregular influence imposed on the system from the environment to which it is coupled. Noise will cause the system to fluctuate. The way these fluctuations evolve as the system undergoes a transition may provide clues to the nature of the underlying bifurcation. Wiesenfeld<sup>3</sup> has recently published a series of papers analyzing the effect of fluctuations on the power spectra of systems close to the bifurcation of limit cycles. The fluctuations add features to the spectra which are characteristic of the impending bifurcation.

In Sec. II we analyze the influence of fluctuations on

the imperfect pitchfork bifurcation. In particular, we look closely at two limiting cases of simpler bifurcations embedded in the unfolding of the pitchfork: the transcritical and the hysteresis bifurcations. These latter are the lowest codimension bifurcations (codimension 1) that mediate continuous transitions between steady states, and they are expected to arise frequently as limiting cases in the unfolding of more complex bifurcations. The pitchfork bifurcation itself is the only codimension 2 bifurcation that mediates a continuous transition between steady states, and it arises frequently in the context of physical systems. It is at the basis of the Landau model of phase transitions and mean-field theory<sup>4</sup> and numerous applications exist to both equilibrium and nonequilibrium transitions in physical systems.<sup>5</sup> An extension to spatially distributed systems is the Ginzburg-Landau equation.

In Sec. III we apply our analysis of the noisy pitchfork bifurcation to data reported on a transition between two turbulent superfluid states, T-I and T-II, observed in liquid-helium counterflow.<sup>6,7</sup> For recent reviews of superfluid turbulence see Ref. 8. Fluctuations in turbulent superfluid helium II were first observed by Hoch *et al.*<sup>9</sup> An analysis of noise on the Vinen equation, which models the laminar-turbulent transition in liquid-helium II, has been provided by Northby,<sup>10</sup> and by Moss and Welland.<sup>11</sup> A microscopic theory exists for the state T-II,<sup>12</sup> treating the turbulence as a homogeneous tangle of quantized vortex lines. No such successful treatment is available for the state T-I. We will show that the normal form of an imperfect pitchfork bifurcation, with noise, provides a very satisfactory model for the turbulent counterflow in the neighborhood of the T-I–T-II transition. Our description of this transition is purely phenomenological, but it provides a unified explanation for steady state, relaxation time, and fluctuation data.

## II. ANALYSIS OF AN IMPERFECT PITCHFORK BIFURCATION WITH WEAK NOISE

In this paper we will only deal with transitions between steady states. As already mentioned in the Introduction, singularity theory provides a complete description of the different possibilities in this case. Bifurcations are categorized according to a measure of their complexity called the codimension. Following the terminology of Golubitsky and Schaeffer,<sup>1</sup> a bifurcation has codimension 0 if a singular point, i.e., a steady state at which the Jacobian of the system becomes singular, will typically be encountered as some distinguished parameter  $\lambda$  is varied, without the need to adjust any secondary parameters. The only codimension 0 bifurcation of steady states is the limit point. This simple example occurs in a hysteresis loop, as shown in Fig. 1. A bifurcation has codimension 1 if it is necessary to adjust a single secondary parameter to a particular value in order to encounter the singularity. A bifurcation has codimension 2 if it is necessary to adjust two such parameters. An infinite hierarchy of bifurcations exists with increasing codimension. However, as the codimension increases, more and more parameters must take on particular values for the bifurcation to be encountered as the distinguished parameter  $\lambda$  is varied; in

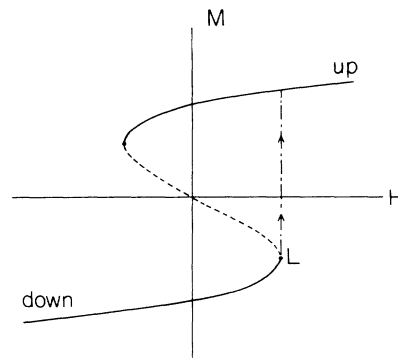


FIG. 1. Ferromagnetic hysteresis loop. The magnetization  $M$  on the ordinate depends on the external field  $H$  given by the abscissa. If  $M$  initially points downward an increasing field  $H$  shifts the magnetization to the right along the lower branch of the curve until the limit point “L” is reached. At L the lower branch loses stability and the magnetization switches discontinuously to the “up” branch.

this sense they are less and less likely to occur in practice. Here we will consider the only codimension 2 bifurcation which mediates a continuous transition between steady states, namely the pitchfork bifurcation. And this bifurcation contains in its unfolding the transcritical and hysteresis bifurcations which are the only codimension 1 bifurcations giving rise to continuous transitions between steady states.<sup>1</sup>

Many different mathematical models contain a given bifurcation. It can be shown that all of these models are in some sense equivalent to certain polynomials, called normal forms. A normal form for the pitchfork bifurcation is  $g(x, \lambda) = -\lambda x - x^3$ . Signs are chosen so that the well-known “pitchfork” diagram of steady states, given by the roots of  $g(x, \lambda) = 0$ , opens out to the left. This choice anticipates the application to liquid-helium counterflow described in Sec. III. In the normal form,  $x$  characterizes the state of the system and  $\lambda$  is the distinguished parameter, the “bifurcation parameter.” The variable  $x$  will generally denote the deviation from some reference state and may thus be positive or negative.

As already mentioned the pitchfork has codimension 2. So two auxiliary parameters must in general be adjusted in order to achieve the singularity at  $g(x=0, \lambda=0)$ . Small perturbations will generally destroy this singularity. Close to the singularity, it can be shown that all analytic perturbations are equivalent to those generated by two terms with coefficients  $\alpha_0$  and  $\alpha_2$  in the “universal unfolding” of the normal form  $g(x, \lambda)$ :

$$p(x, \lambda) = \alpha_0 - \lambda x + \alpha_2 x^2 - x^3. \quad (1)$$

Steady states of the unfolded bifurcation are given by  $p(x, \lambda) = 0$  and the dynamics are modeled close to the singularity by  $\dot{x} = p(x, \lambda)$ . When  $\alpha_0$  and  $\alpha_2$  have nonzero values, a continuous transition between steady states will still be made. However, no singular point will be encountered, the stable steady state will retain its linear stability

through the transition region. Such a transition is known as an "imperfect" bifurcation. In order to avoid cumbersome terminology, we will refer to  $p(x, \lambda)$  itself as the normal form of the pitchfork bifurcation.

Following Golubitsky and Schaeffer, we depict the unfolding of the pitchfork bifurcation graphically by showing bifurcation diagrams for various values of the secondary parameters, see Fig. 2. A bifurcation diagram for the pitchfork is a plot of the roots of  $p(x, \lambda)$  as a function of the bifurcation parameter  $\lambda$ . We restrict our analysis to the domain below the abscissa  $\alpha_0 = 0$  and to the right of the curve  $\alpha_0 = \alpha_2^3/27$ . Here a continuous curve of roots  $x_-(\lambda)$  with negative values of  $x$  exists for  $-\infty < \lambda < \infty$ . We consider the negative roots because these apply most naturally to the liquid-helium model discussed in Sec. III. However, the bifurcation diagrams in the other domains of the  $(\alpha_2, \alpha_0)$  parameter plane are either related to those we consider by reflection about the axis  $x = 0$  or else contain discontinuous transitions with which we are not concerned.

The perfect pitchfork bifurcation is at the origin of the  $(\alpha_2, \alpha_0)$  parameter plane, where the two auxiliary parameters are equal to a particular numerical value, namely zero. The axis  $\alpha_0 = 0$  is a line of codimension-1 transcritical bifurcations. The curve  $\alpha_0 = \alpha_2^3/27$  is the loci of codimension-1 hysteresis bifurcations.

Imperfect bifurcations occur in the unfolding of the pitchfork as Fig. 2 illustrates. If  $\alpha_2 > 0$  then these imperfect bifurcations will have the character of imperfect transcritical bifurcations locally about the origin  $(x, \lambda) = (0, 0)$  of the bifurcation diagram. If  $\alpha_2 < 0$  they will have the character of imperfect hysteresis bifurcations. When the

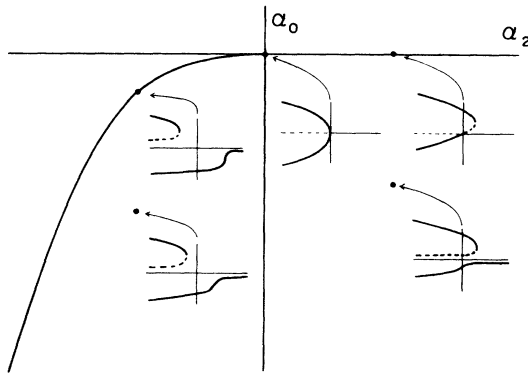


FIG. 2. Bifurcation diagrams within the unfolding of the pitchfork bifurcation for different values of the parameters  $\alpha_0$  and  $\alpha_2$ . Shown is the domain below the abscissa  $\alpha_0 = 0$  and to the right of the curve  $\alpha_0 = \alpha_2^3/27$ . The codimension-2 pitchfork bifurcation is at the origin of the  $(\alpha_2, \alpha_0)$  parameter plane. The axis  $\alpha_0 = 0$  is a line of codimension-1 transcritical bifurcations. The curve  $\alpha_0 = \alpha_2^3/27$  is the loci of codimension-1 hysteresis bifurcations.

deviation of the secondary parameters from the particular values necessary for a singularity is indeed small, then the system will pass, as the bifurcation parameter  $\lambda$  is varied, through a region of weakened linear stability. This region will be a neighborhood of the singular point in the product space of state variables and parameters. In this region the magnitude of fluctuations of the state variable and their relaxation times will be enhanced. However, since no true singularity is encountered, the relaxation times will always remain finite, i.e., fluctuations will decay exponentially. We shall call the point on the bifurcation diagram at which the relaxation time reaches its greatest value the "paracritical" point, and we will denote it  $(x_p, \lambda_p)$ .

A general system containing a pitchfork bifurcation will not necessarily have the form (1). However, there will exist in general a smooth change of coordinates which maps the steady states of the model system onto those of the normal form in some neighborhood of the origin  $(x, \lambda) = (0, 0)$ . Only in this neighborhood can properties of a given model be inferred from those of the normal form.

Much may be learned about the dynamics of a system undergoing a bifurcation by analyzing fluctuations. Wiesenfeld has thoroughly studied fluctuations in systems bifurcating from limit cycles.<sup>3</sup> Here we analyze fluctuations associated with imperfect bifurcations between steady states. Our approach has been motivated by a series of experiments on the transition between two steady states of superfluid turbulence in liquid helium reported by Griswold, Lorenson, and Tough.<sup>6,7</sup> Fluctuations about the steady state were studied as a function of the bifurcation parameter. We consider a model whose deterministic part is based on the normal form (1) and which includes two sources of noise:<sup>13,14</sup>

$$dx = [\alpha_0 - (\lambda - z)x + \alpha_2 x^2 - x^3]dt + \sigma_1 dW_1$$

$$= p(x, \lambda)dt + \sigma_1 dW_1 + xz dt, \quad (2)$$

$$dz = -\gamma z dt + \sigma_2 dW_2. \quad (3)$$

This model contains the two sources of noise any non-equilibrium system will inevitably be subject to. Namely internal noise or thermal noise which represents the influence of the large number of (microscopic) degrees of freedom on the behavior of the systems. Internal noise generally evolves on a time scale very fast compared to the time scale of the system and is thus usually modeled by an additive Gaussian white noise. This is the term  $\sigma_1 dW_1$  in (2). Nonequilibrium systems are open systems and as such coupled to an environment. The fluctuations in the environment are a second source of noise for the system. The effect of these fluctuations on a nonlinear system is often state dependent, for instance if they give rise to noise in the bifurcation parameter. In our model this leads to the linear term  $xz dt$ , modeling a source of random disturbances perturbing the bifurcation parameter. Since the ratio of the time scales of the system and the external noise can change as the paracritical point is approached, we have chosen to represent this linear noise by a Gaussian process with a nonvanishing correlation time, namely an Ornstein-Uhlenbeck process (OU noise)

with correlation time  $\gamma^{-1}$ . This allows us to describe the competition between the two time scales close to the paracritical point  $x_p$ .

The intensity of internal fluctuations generally scales with an inverse power of the system's size and these fluctuations are thus usually a weak source of disturbance in macroscopic systems. Obviously external noise (unless deliberately applied) is usually also weak in the laboratory experiments. Weak noise will give rise to Gaussian fluctuations in the state variable with small amplitude about the deterministic steady state. If we expand (2) about the deterministic steady state using  $x = x_- + y$ , and then linearize, we obtain the system

$$d \begin{pmatrix} y \\ z \end{pmatrix} = \begin{pmatrix} p'_s(\lambda) & x_- \\ 0 & -\gamma \end{pmatrix} \begin{pmatrix} y \\ z \end{pmatrix} dt + \begin{pmatrix} \sigma_1 & 0 \\ 0 & \sigma_2 \end{pmatrix} \begin{pmatrix} dW_1 \\ dW_2 \end{pmatrix}, \quad (4)$$

where

$$p'_s(\lambda) = (d/dx)p(x, \lambda) \Big|_{x=x_-(\lambda)} = -\lambda + 2\alpha_2 x_- - 3x_-^2. \quad (5)$$

The solution to this system of linear stochastic differential equations is indeed a Gaussian random process. The variance  $\langle y^2 \rangle$  about the steady state  $x_-(\lambda)$  is given by the sum of two terms, one due to the additive internal fluctuations and the other due to the linear noise<sup>14</sup>

$$v = v_1 + v_2, \quad v_1 = \frac{\sigma_1^2}{2|p'_s|}, \quad v_2 = \frac{x_-^2 \sigma_2^2}{2|p'_s| \gamma(\gamma - p'_s)}. \quad (6)$$

As indicated by the form of (6), our expression for the variance does not depend on the explicit form of  $p(x, \lambda)$ . Equation (6) gives the variance for stable steady states weakly perturbed by additive white noise and an independent linear OU noise; the normal form  $p(x, \lambda)$  is arbitrary. Thus (6) applies not only to the pitchfork bifurcation, but also, for instance, to the transcritical or hysteresis bifurcations.

In Eq. (6), the term  $v_1$  due to internal fluctuations is inversely proportional to the restoring force  $p'_s$  back to the deterministic steady state. Near a singular point, where  $|p'_s|$  is small, we have the familiar phenomenon of enhanced critical fluctuations. The term  $v_2$  due to linear noise is more complex; in order to understand it better we first discuss the limit corresponding to short correlation times  $\gamma^{-1}$ . Below we will also discuss the long correlation time limit.

The short correlation time limit is obtained by substituting  $\gamma \rightarrow \epsilon^{-2}\gamma$  and  $\sigma_2 \rightarrow \epsilon^{-1}\sigma_2$  in the second component of Eq. (4) and  $xz dt \rightarrow \epsilon^{-1}xz dt$  in the first component of Eq. (4), and then taking the limit  $\epsilon \rightarrow 0$ .<sup>13</sup> We obtain for the variance due to external noise

$$v_2 = \frac{x_-^2 \sigma_2^2}{2\gamma^2 |p'_s|} \rightarrow \frac{x_-^2 \sigma_2^2}{2|p'_s|}, \quad \frac{\sigma_2^2}{\gamma^2} \rightarrow \sigma_2^2. \quad (7)$$

We would obtain the same expression by first substituting  $xz dt \rightarrow \sigma x dW_2$  in (2) and linearizing

$$dy = p'_s(\lambda)y dt + \sigma_1 dW_1 + \sigma_2 x_- dW_2. \quad (8)$$

The variance then calculated directly from (8) agrees with (7). The form of (7) is easy to understand.  $v_2$  is quadratically dependent on  $x_-$ , reflecting the fact that the noise strength is linear in  $x_-$  and the variance is a mean-square deviation. As with the contribution due to additive noise, the variance is also inversely proportional to the strength of the restoring force  $p'_s$ .

When the variance of fluctuations on a state variable is given as a function of  $\lambda$ , what can we deduce about the parameter values in the underlying normal form (2)? We will see that something may be learned by analyzing (6) to find out when the two components  $v_1$  and  $v_2$  contribute distinct maxima to the envelope of the sum. We consider first the analytically tractable case of the white noise perturbing the pitchfork bifurcation. We will then compare these results with those obtained numerically for the more complicated case of colored noise.

Adding the short correlation time limit (7) for linear noise to the contribution  $v_1$  in (6) due to additive noise and differentiating with respect to  $\lambda$ , we obtain the extremum condition for white noise:

$$0 = \frac{dV}{d\lambda} = \frac{2\sigma_2^2 x_- (dx_-/d\lambda) |p'_s| + (\sigma_1^2 + \sigma_2^2 x_-^2) (dp'_s/d\lambda)}{2|p'_s|^2}. \quad (9)$$

The denominator is strictly positive and therefore the extremum condition may be analyzed by considering the numerator alone. We will proceed by obtaining expressions for  $|p'_s|$ ,  $dp'_s/d\lambda$ , and  $dx_-/d\lambda$  in terms of the independent variable  $x_-$  alone, eliminating  $\lambda$ . However,  $x_-$  is a monotonic function of  $\lambda$ . Thus the zeros of  $dV/d\lambda$  expressed as a function of  $x_-$ , for  $x_-$  negative, are in one-to-one correspondence with those of  $dV/d\lambda$  expressed as a function of  $\lambda$ .

The expression for  $p'_s(\lambda)$  is given by (5), and therefore

$$\frac{dp'_s(\lambda)}{d\lambda} = -1 + 2\alpha_2 \frac{dx_-}{d\lambda} - 6x_- \frac{dx_-}{d\lambda}. \quad (10)$$

To obtain an expression for  $dx_-/d\lambda$  we note that  $x_-(\lambda)$  is a root of  $p(x, \lambda) = 0$  so that we have the identity  $p(x_-(\lambda), \lambda) = 0$ . Then on differentiating

$$0 = dp(x_-(\lambda), \lambda)/d\lambda = (\partial p/\partial x_-) dx_-/d\lambda + \partial p/\partial \lambda = p'_s(\lambda) dx_-/d\lambda + x_-, \quad (11)$$

from which

$$dx_-/d\lambda = x_- / |p'_s(\lambda)|. \quad (12)$$

From  $p(x_-(\lambda), \lambda) = 0$  we solve for  $\lambda$ ,

$$\lambda = \alpha_0 x_-^{-1} + \alpha_2 x_- - x_-^2. \quad (13)$$

Substituting (13) into (5) and the result into (11) we then have

$$dx_-/d\lambda = x_-^2 (-\alpha_0 + \alpha_2 x_- - 2x_-^3)^{-1}. \quad (14)$$

Substituting (5), (10), and (14) into the numerator of (9) and assuming that  $\alpha_2, \sigma_2 \neq 0$  we obtain the following cri-

terion for extrema in the variance considered as a function of  $\lambda$ :

$$Q(x_-) = D \text{ where } Q(x_-) = x_-^2(x_-^2 + Bx_- + C), \tag{15}$$

and

$$B = 4\alpha_2^{-1}r^2, \quad C = -(3\alpha_0\alpha_2^{-1} + r^2), \quad D = \alpha_0\alpha_2^{-1}r^2, \tag{16}$$

where  $r \equiv \sigma_2/\sigma_1$ .

Our analysis now separates into two cases: that of the hysteresislike imperfections with  $\alpha_2 < 0$ , and that of the transcriticallike imperfections with  $\alpha_2 > 0$ . We begin with the hysteresislike case. Then we have

$$\alpha_0 < 0 \text{ and } \alpha_2 < 0 \implies B < 0, \quad C < 0, \quad D > 0. \tag{17}$$

The sign of  $C$  indicates that we have a quadratic maximum of  $Q(x_-)$  at the origin. We also note that  $Q(x_-) \rightarrow \infty$  as  $|x_-| \rightarrow \infty$ . Since a fourth-order polynomial has at most three extrema, we must therefore have the qualitative picture shown in Fig. 3(a). We see that there will be exactly one intersection of  $Q(x_-)$  with the constant line  $x_- = D$  in the physical domain  $x_- < 0$ . This intersection corresponds to a unique value of  $\lambda$  for which  $dV/d\lambda = 0$ .  $V(\lambda)$  is strictly positive and it is easy to show

that  $V(\lambda) \rightarrow 0$  as  $\lambda \rightarrow \infty$ . Therefore, the unique extremum must correspond to a maximum in the variance. We show this result on the  $(\alpha_2, \alpha_0)$  parameter plane in Fig. 4. To the left of the  $\alpha_0$  axis and below the curve of hysteresis bifurcations  $\alpha_0 = \alpha_2^3/27$ , we have a domain where the variance diagram has only a single maximum.

In the transcriticallike case,  $\alpha_2$  is positive so that we have

$$\alpha_0 < 0 \text{ and } \alpha_2 > 0 \implies B > 0 \text{ and } D < 0, \tag{18}$$

however the sign of  $C$  is indeterminate. Depending on the sign of  $C$ , we may have either a quadratic maximum or minimum at the origin. The graph of  $Q(x_-)$  for these two cases is shown in Fig. 3(b). In either case extrema in the variance diagram correspond to intersections of the graph with the constant line  $Q(x_-) = D$  for  $x_- < 0$ . We see that for transcriticallike imperfections we will in general have either zero or two intersections. Between these two generic cases we have the critical case of only a single intersection, as is shown in the figure. We would like to calculate the bifurcation set of the variance diagram, that is, the loci of the critical case in the  $(\alpha_0, \alpha_2)$  parameter plane. In this situation we have  $Q(x_c) = D$ , where  $x_c$  is the coordinate of an extreme value of  $Q(x)$ , satisfying  $Q'(x_c) = 0$ . One root of this equation is at the origin and the other two roots are given by

$$x_c = \frac{3}{8}[-B \pm (B^2 - \frac{32}{9}C)^{1/2}]. \tag{19}$$

Then  $Q(x_c) = D$  leads directly to

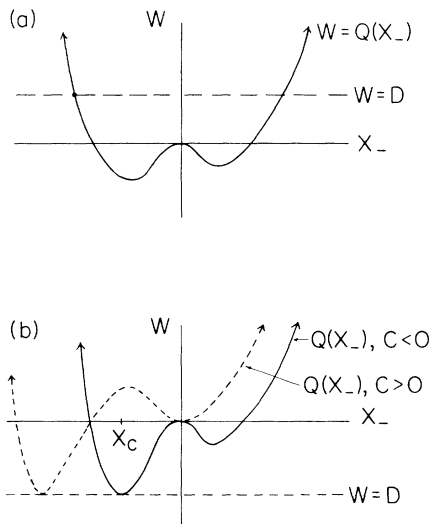


FIG. 3. Graphs of the function  $Q(x_-)$  for the case of (a) hysteresislike and (b) transcriticallike imperfections. For hysteresislike imperfections there will always be one solution to  $Q(x_-) = D$  for the physical case of  $x_- < 0$ . For transcriticallike imperfections there are two ways that the graph of  $Q(x_-)$  may be drawn, depending on whether  $C$  is positive (dashed line) or negative (solid line). In either case there are generally no real solutions or else two real solutions to  $Q(x_-) = D$  for  $x_- < 0$ . The critical situation in which a minimum of  $Q(x_-)$  is tangent to  $w = D$  is depicted.  $x_c$  is the coordinate of the physical minimum of  $Q$ , and is shown for the case of  $C < 0$ .

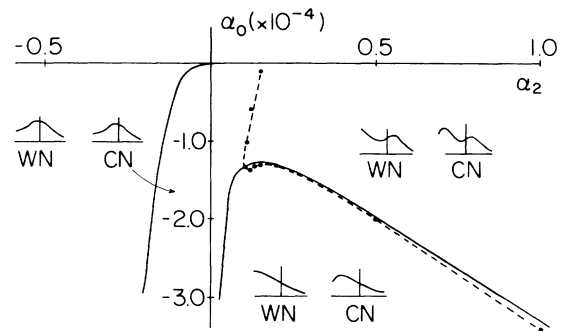


FIG. 4. Bifurcation set of the imperfect pitchfork variance diagrams for white and colored noise. Sketches of the variance diagram are shown in each domain of the unfolding of the pitchfork. Variance diagrams for white noise are labeled WN, those for colored noise are labeled CN. In the white-noise case the line  $\alpha_2 = 0$  separates hysteresislike diagrams with a single extremum from transcriticallike diagrams with two extrema. A root of Eq. (21) gives the solid line in the transcriticallike domain, which separates two extrema diagrams from zero extrema diagrams. The bifurcation set for colored noise is represented by the dashed line which was interpolated between the numerically observed points (●). Colored noise results in an additional maximum for each diagram in the transcriticallike domain.

$$(B^2 - \frac{32}{9}C)^{1/2}(-9B^2 + 32BC) = 27B^4 + 128C^2 - 144B^2C + 512D . \quad (20)$$

After squaring both sides and introducing the definitions (16), we group terms of like powers in  $\alpha_0$  and finally arrive at the condition

$$0 = 81\alpha_2\alpha_0^4 + (180\alpha_2^2r^2 + 108r^4)\alpha_0^3 + (118\alpha_2^3r^4 + 540\alpha_2r^6)\alpha_0^2 + (20\alpha_2^4r^6 + 180\alpha_2^2r^8 + 432r^{10})\alpha_0 + 4\alpha_2^3r^{10} + \alpha_2^5r^8 . \quad (21)$$

The roots of this polynomial as a function of  $\alpha_0$  give the bifurcation set for extrema of the variance diagram in the  $(\alpha_0, \alpha_2)$  plane. Figure 4 shows the roots for the case  $r=0.5$ , corresponding to the relative strengths of linear and additive noise used in our discussion of the application to liquid helium below. A second curve of real roots to (21) also exists in this case; this is not shown because these roots correspond to unphysical positive values of  $x_-$ . In addition, the polynomial has a pair of complex-conjugate roots for the range of values of  $\alpha_0$  shown.

Sketches of the variance diagram are shown for each domain in the figure. They are labeled “WN” for white noise. Above the bifurcation set the variance diagrams have two extrema. As  $\lambda \downarrow -\infty$  the variance increases monotonically to its limiting value of  $\sigma_2^2/4$ . Below the bifurcation set there are no extrema at all. The axis  $\alpha_2=0$  is also a bifurcation set, dividing the transcriticallike case of two extrema from the hysteresislike case with only a single extremum.

Our analysis has thus far been concerned with the white-noise limit, in which the correlation time of the noise disturbing the system is assumed to be much shorter than the time associated with deterministic relaxation back to the steady states:  $\gamma^{-1} \ll p_s'(\lambda_p)^{-1}$ . Close to the paracritical point, and for sufficiently small  $|\alpha_0|$  and  $|\alpha_2|$ , we expect that this relaxation time will be large and so the assumption holds. But for large  $|\lambda|$  the relaxation time decreases as  $|\lambda|^{-1}$  and eventually the white-noise approximation will be inappropriate. Another limit of interest is the long correlation time limit,  $\gamma^{-1} \gg p_s'(\lambda)^{-1}$ , where once again the expression for the variance simplifies.

Formally, the long correlation time limit is obtained by substituting  $\gamma \rightarrow \epsilon^2\gamma$  and  $\sigma_2 \rightarrow \epsilon\sigma_2$  in the system (4) and taking  $\epsilon \rightarrow 0$ . Using this limit, the total power of the noise processes remains finite.<sup>13(b)</sup> The resultant expression for the variance  $v_2$  is given by

$$v_2 \rightarrow \frac{x_-^2 \sigma_2^2}{2\gamma |p_s'|^2} . \quad (22)$$

This result may be understood by means of the following intuitive argument. If the correlation time of the noise process is much greater than the relaxation time to the deterministic steady state, then the system will always be quasistationary with respect to the slowly changing value of the effective bifurcation parameter  $\lambda+z$  in (2). As a

consequence we expect the amplitude of fluctuations in  $x$  to be related to those in  $\lambda$  through  $\sigma_x = (dx_-/d\lambda)\sigma_\lambda$ ; see Fig. 5. The variance in  $\lambda$  is that of the Ornstein-Uhlenbeck process (3);  $\sigma_\lambda^2 = \sigma_z^2 = \sigma_2^2/2\gamma$ . Using (12) we then obtain

$$\sigma_x^2 = \left[ \frac{dx_-}{d\lambda} \right]^2 \frac{\sigma_2^2}{2\gamma} = \frac{x_-^2 \sigma_2^2}{2\gamma |p_s'|^2} , \quad (23)$$

in agreement with (22).

We note that the general form for the variance  $v_2$  in (6) interpolates between the long correlation time limit (22) and the short correlation time limit (7) via the denominator  $(\gamma - p_s')$ . The short correlation time limit is taken by only keeping the second term in the denominator and the long correlation time limit is obtained by only keeping the first.

To illustrate the difference between the long and short correlation time limits consider the perfect pitchfork  $p(x, \lambda) = -\lambda x - x^3$ . For  $\lambda < 0$  the long correlation time limit leads to  $v_2 = \sigma_2^2(8|\lambda|\gamma)^{-1}$  and the white-noise limit gives  $v_2 = \sigma_2^2/4$ . When the pitchfork is imperfect the behavior for large  $|\lambda|$  is qualitatively the same; the effect of finite correlation times is to decrease the variance in proportion to  $|\lambda|^{-1}$  as  $\lambda \downarrow -\infty$ . The effect of finite correlation times on variance diagrams for transcriticallike imperfections is then to add an additional maximum value in the variance, where for more negative values of  $\lambda$  the variance decreases to zero. Finite correlation times do not modify the number of extrema in the case of hysteresislike imperfections, where even for white noise the variance decreases asymptotically as  $\lambda \downarrow -\infty$ . Sketches of the variance diagrams for colored noise (labeled “CN”) are shown next to those for white noise in Fig. 3.

What is the effect of finite correlation times in the bifurcation set shown in Fig. 4? This has been investigated numerically by computing a series of variance diagrams for fixed  $\alpha_2$  while varying  $\alpha_0$ , and recording the critical value of  $\alpha_0$  where the number of extrema visibly change. The dashed line in the figure interpolates between our observations. The bifurcation set for finite correlation times follows closely the one for white noise along the branch furthest from the axis  $\alpha_2=0$ . Here the white-noise ideal-

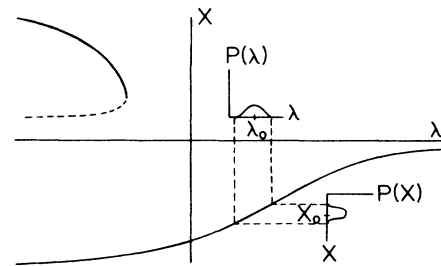


FIG. 5. When the system relaxation time  $|p_s'(\lambda)|^{-1}$  is much shorter than the external noise correlation time  $\gamma^{-1}$ , the state variable  $x$  closely follows the slowly changing values of the effective bifurcation parameter  $\lambda+z$ :  $x_t \approx x_-(\lambda+z)$ .

zation is apparently robust with respect to the exact character of the noise so long as the correlation time of the noise is much shorter than the relaxation time of the system in the neighborhood of the paracritical point. However, close to this axis the results for white noise diverge sharply from those for finite correlation times. In this region the extrema are due to a shallow modulation of the variance which rises quickly towards its asymptotic value as  $\lambda$  decreases. The number and position of the extrema are here very sensitive to small changes in the character of the noise.

### III. APPLICATION TO LIQUID HELIUM

Griswold, Lorenson, and Tough<sup>6,7</sup> have studied the transition between two superfluid turbulent states in liquid helium. Their apparatus includes a reservoir of liquid helium connected to a small chamber with a heater by means of a thin flow tube. A pressure transducer in the chamber measures the pressure difference across the flow tube, which is proportional to the chemical potential difference  $\Delta G$  across the tube. This chemical potential difference is a state variable and may be related to the vortex line density in the superfluid flowing through the tube. The behavior of the state variable is measured as a function of  $\dot{Q}$ , the rate at which heat is introduced into the helium by the heater. According to the two fluid model the flow through the tube may be treated as a counterflow of two fluids; the superfluid component flowing from the reservoir to the heater and the normal fluid component flowing in the opposite direction. For low values of  $\dot{Q}$  the chemical potential difference  $\Delta G = 0$ . At a critical value of  $\dot{Q}$ ,  $\Delta G$  increases discontinuously to a finite value. This transition is associated with the appearance of quantized vortices in the superfluid. The resultant turbulent state is denoted T-I. As  $\dot{Q}$  is further increased the state T-I undergoes a complex transition to another superfluid turbulent state: T-II.

Turbulent superfluid states T-I and T-II and the transition region between them all consist of macroscopic steady states. The simplest transitions between macroscopic steady states are one state variable bifurcations. Certain transitions between steady states do have more than one state variable in their normal form, however, these all have codimension 3 or greater.<sup>1</sup> In this sense they are less likely to be encountered. Therefore, it is quite natural to attempt to model the transition between T-I and T-II using only a single-state variable. Furthermore, we know that in the case of superfluid helium many properties of states T-I and T-II are successfully described by a phenomenological one-state variable theory based on the Vinen equation.

We suggest that the transition between states T-I and T-II takes place via an imperfect pitchfork bifurcation perturbed by both additive and linear multiplicative noise. This interpretation provides a qualitative explanation for results of steady state, fluctuation, and relaxation time measurements. First we will describe the results expected on the basis of our model in the transcriticallike and hysteresislike regimes. Then we will compare these with the experimental results reported by Griswold *et al.*<sup>7</sup> at 1.6

and 1.75 K. We will see that the measurements at 1.6 K agree more closely with the transcriticallike case, while the measurements at 1.75 K resemble the hysteresislike case.

We now proceed to describe the results of our model in the near transcritical limit. Figures 6(a) and 6(b) show a bifurcation diagram in the regime  $\alpha_2 > 0$  and

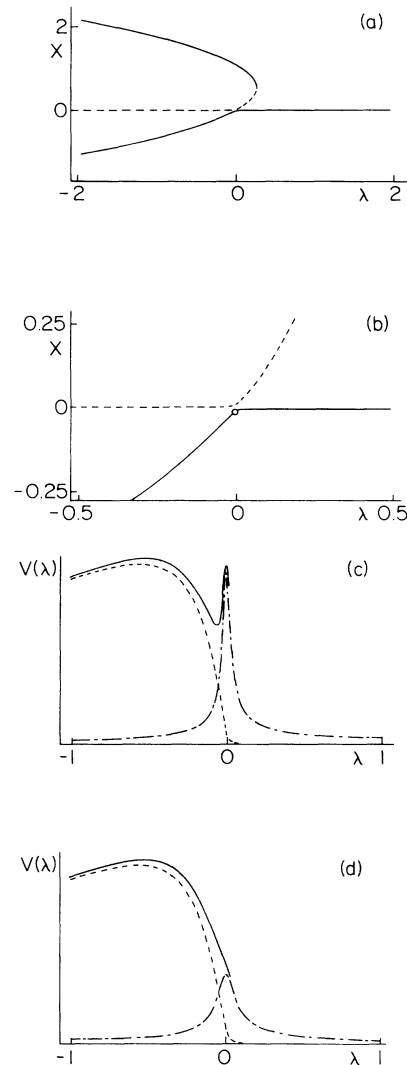


FIG. 6. Imperfect transcritical bifurcation in the unfolding of the pitchfork. (a) Global view of the bifurcation diagram  $\alpha_0 = -1 \times 10^{-4}$ ,  $\alpha_2 = 1$ . (b) Magnified view of a small region near the origin. The small circle (O) is centered around the paracritical point. (c) Variance as a function of  $\lambda$  for the same values of  $\alpha_0$  and  $\alpha_2$ , and with  $r = 0.5$ . The envelope of  $v_1$  (— · — · —) is roughly centered at the origin. The envelope of the linear component  $v_2$  (— — —) rises to the left, where the pitchfork opens up. Also shown is the summed envelope  $v = v_1 + v_2$  (—). The additive component contributes a distinct peak in the envelope for the total variance. (d) Variance as a function of  $\lambda$  for parameter values  $\alpha_0 = -6 \times 10^{-4}$ ,  $\alpha_2 = 1$ , and  $r = 0.05$ . The additive component is not resolved in the envelope of the total variance.

$|\alpha_0/\alpha_2| \ll 1$ , near a transcritical bifurcation. Figure 6(a) provides a global view and 6(b) magnifies a small neighborhood of the origin. The lower curves represent stable steady states and are the ones we label  $x_-$ . In Figure 6(b) a small circle is drawn around the paracritical point  $(x_p, \lambda_p)$ ; it occurs close to the point of maximum curvature of  $x_-(\lambda)$ .

Figure 6(c) displays the variance (6) as a function of  $\lambda$ , with the same parameter values  $\alpha_0$  and  $\alpha_2$  as were used to generate 6(a) and 6(b). Both the components  $v_1$  and  $v_2$  and the total variance are shown. Note that according to (6),  $v_1$  is proportional to the deterministic relaxation time  $|p'_s|^{-1}$ , reaching its maximum value at the paracritical point.  $v_1$  peaks near  $\lambda=0$  and  $v_2$  rises to the left. A shoulder appears in the envelope for the total variance with a maximum corresponding to  $v_1$ . Figure 6(d) has the same parameters as 6(c) except for a larger value of  $|\alpha_0|$ ; in this case the shoulder is not resolved in the envelope of the total variance.

Figure 7 displays a bifurcation diagram for parameter values near the curve of hysteresis bifurcations given in Fig. 2. The paracritical point is now close to the inflection point in the curve  $x_-(\lambda)$ . Figure 7(b) shows the corresponding plots of variance versus  $\lambda$ . The maxima of  $v_1$  and  $v_2$  are only slightly separated and both close to the paracritical point. The total variance shows only a single peak with no hint of separate components.

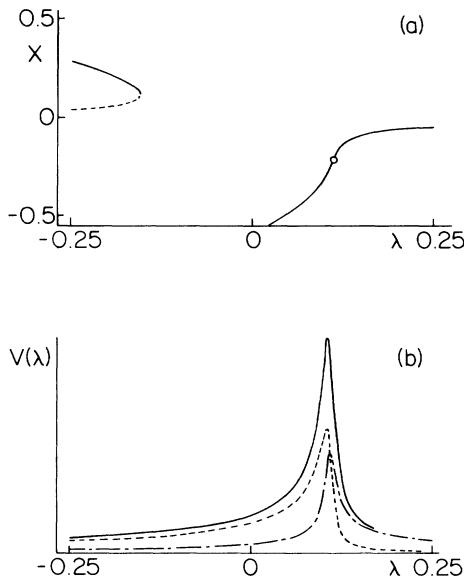


FIG. 7. Imperfect hysteresis bifurcation in the unfolding of the pitchfork. (a) Bifurcation diagram for  $\alpha_0 = -8.6 \times 10^{-3}$ ,  $\alpha_2 = 0.5$ . The small circle ( $\circ$ ) is centered around the paracritical point of  $x_-$ . (b) Variance as a function of  $\lambda$  for the same parameter values. Both the additive (— · — · —) and linear (— — —) components peak near the inflection point of the bifurcation diagram. The summed envelope (—) has only a single maximum.

We now turn to the measured steady states, relaxation times, and fluctuation power as reported by Griswold *et al.*<sup>7</sup> Figure 8(a) shows the measured loci of turbulent superfluid steady states as a function of the parameter  $\dot{Q}$  in the regime of the T-I to T-II transition at 1.6 K. The transition has a complex global structure. The normal form (1) represents a power-series expansion of the pitchfork bifurcation about the singular point, which is close to the paracritical point. Therefore, we only claim to model the transition in some neighborhood of the empirical paracritical point, which is denoted “c” in Fig. 8(a). To the

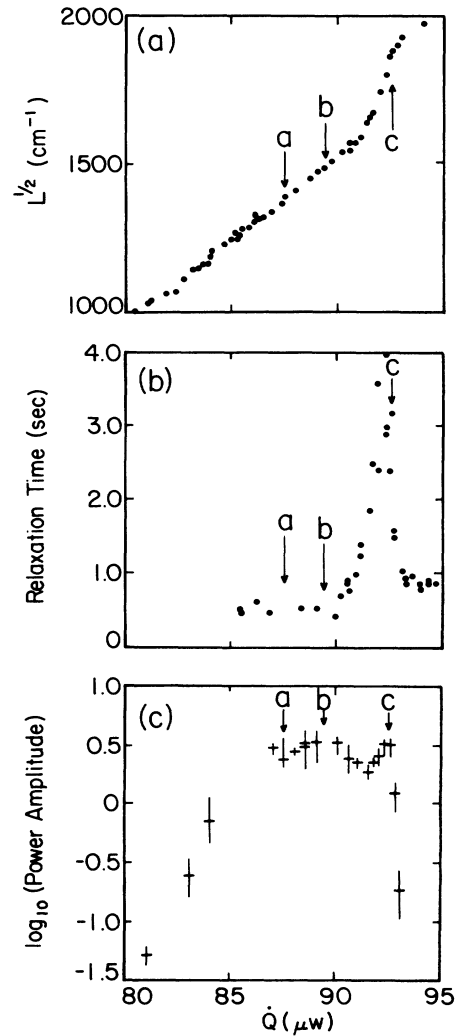


FIG. 8. Measured properties of liquid-helium counterflow at 1.6 K (Ref. 7). (a) Steady-state values of the free energy across the flow tube as a function of the heat current  $\dot{Q}$  in the T-I to T-II transition region. The paracritical point is marked c. (b) The relaxation time as a function of heat current in the T-I and T-II transition region. The relaxation time reaches a maximum at the paracritical value of  $\dot{Q}$ . (c) The power at 0.1 Hz of fluctuations in the T-I and T-II transition region. At the paracritical value of  $\dot{Q}$  there is a local maximum. Adapted from Ref. 7.

right of  $c$ , a line of steady states extends into the T-II region; these we associate with the line of trivial steady states extending to the right of the paracritical point of Fig. 6(b). The measured power of the fluctuations rapidly decreases to zero as  $\dot{Q}$  is increased into the T-II region, in agreement with our formula for variance as shown in Fig. 6(c).

We locate the empirical paracritical point at the value of  $\dot{Q}$  where the measured relaxation time attains its maximum value, see Fig. 8(b). It is close to the center of the rounded corner in the curve of steady states. This is consistent with our results for the transcritical bifurcation as shown in Fig. 6(a). It is in contrast with the situation of the hysteresis bifurcation shown in Fig. 7(a); in that case the paracritical point is found near the inflection point of the curve of steady states. At the paracritical value of  $\dot{Q}$  there is a local maximum in the fluctuation power, shown in Fig. 8(c), corresponding to the resolved shoulder in the total variance due to additive noise as seen in Fig. 6(c). No such distinct component can be resolved in the total variance of a noisy hysteresis bifurcation. To the left of the paracritical point a curve of steady states descends into the transition region between T-I and T-II. Here the experimentally measured fluctuation power increases to a broad maximum at "b" before decreasing again. Our computed variance also increases as the bifurcation parameter decreases from the paracritical value, due to the contribution of linear noise.

Figure 9(a) shows steady states measured at 1.75 K. Once again the paracritical point is marked  $c$ . As compared with the data given for 1.6 K, the paracritical point is now shifted away from the point of maximum curvature and is closer to the inflection point of the loci of steady states. This resembles the geometry of steady states in our model for the near hysteresis regime. Figure 9(b) shows the relaxation time curve whose maximum determines the location of the empirical paracritical point. Figure 9(c) shows the measured fluctuation power as a function of  $\dot{Q}$ ; this should be compared with the model variance shown in Fig. 7(b). There is no clearly resolved maximum corresponding to the paracritical point; this is also consistent with the near hysteresis limit.

We note that the line of measured steady states which extends to the right of the paracritical point in Figs. 8(a) and 9(a) is not parallel to the axis of the parameter  $\dot{Q}$ . If  $\dot{Q}$  were to change suddenly while the system were in state T-II, the system would be taken away from a steady state. In contrast the line of trivial steady states shown in Fig. 6(b) nearly lies along the  $\lambda$  axis. In this region fluctuations in  $\lambda$  make very little difference to the steady state value of  $x$ , and consequently linear noise makes very little contribution to the variance. In fact, experiments have been performed with the counter-current apparatus in which the heat current was deliberately made to fluctuate.<sup>7</sup> The resulting variance did not decrease as  $\dot{Q}$  increased from  $c$ , but rather grew as  $\dot{Q}^2$ . This demonstrates that the intrinsic fluctuations shown in Fig. 9(c) are not due to fluctuations in  $\dot{Q}$ .

The relationship between the experimental  $(\dot{Q}, L^{1/2})$  coordinates and the  $(\lambda, x)$  coordinates of our model is shown in Fig. 10. Following the standard procedure, we

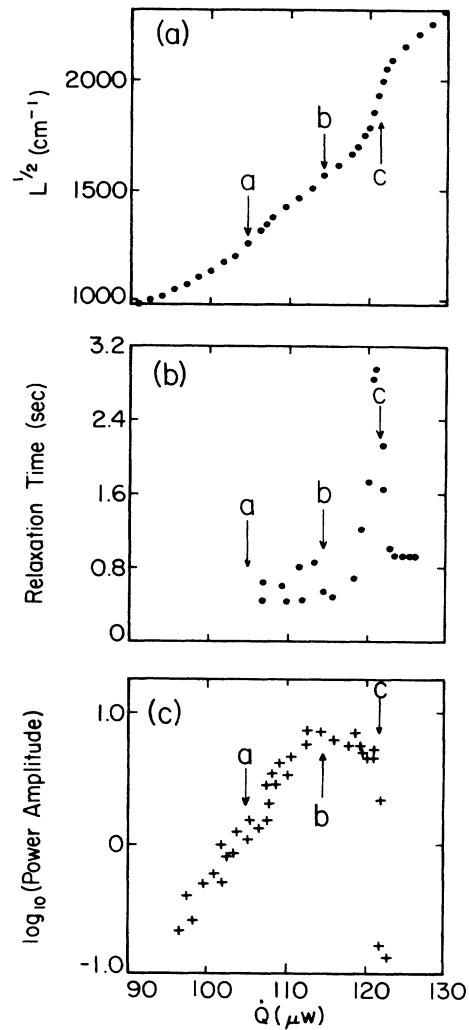


FIG. 9. Measured properties of liquid-helium counterflow at 1.75 K (Ref. 7). (a), (b), and (c) as in Fig. 7. In (a) the paracritical point is shifted towards the inflection point and away from the point of maximum curvature on the curve of steady states, as compared with Fig. 8(a). In (c), no maximum is apparent at the paracritical point. Adapted from Ref. 7.

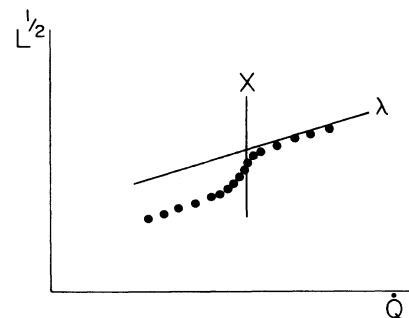


FIG. 10. Relation between model coordinates  $(\lambda, x)$  and experimental coordinates  $(\dot{Q}, L^{1/2})$ .  $\lambda \propto \dot{Q}$  and  $x = L_0^{1/2} - s(\dot{Q} - \dot{Q}_0)$ , where  $s$  is the slope.

transform coordinates so that the line of trivial steady states corresponds to  $\lambda=0$ . The experiments reported in Ref. 7 demonstrate that  $\dot{Q}$  does not itself fluctuate; how can this be compatible with our model of fluctuations in  $\lambda$ ? Suppose we write  $\lambda=\Lambda-\Lambda_0$ , where  $\Lambda=\Lambda_0$  is the singular point. The expression for linear noise  $\lambda+z$  in our model (2) can then be interpreted as due to fluctuations in  $\Lambda_0$ . In other words it may not be the bifurcation parameter that fluctuates but rather the critical point at which the bifurcation takes place. This is one possible interpretation. However, our model is consistent with any source of noise whose amplitude depends linearly on the state variable  $x_-$ .

There is a simple physical explanation for a state-dependent noise which disturbs T-I much more than T-II and which is associated with a bifurcation point  $\Lambda_0$  which fluctuates up and down the line of trivial steady states. Schwarz's theory of homogeneous turbulence has very successfully described the state T-II; therefore, we expect the line of steady states in T-II to be nearly independent of the geometry of the experimental apparatus, and in particular of any irregular influences associated with the walls. However, the state T-I is likely to be inhomogeneous<sup>8</sup> and sensitive to the proximity of the capillary tube walls. The critical heat current at which the transition between T-I and T-II takes place also depends on the geometry of the tube; it is roughly in inverse proportion to the tube diameter.<sup>8(a)</sup> Therefore, any irregularities associated with the wall and the fluid flow close to the wall may strongly perturb state T-I and the transition between T-I and T-II while leaving the steady states of T-II virtually undisturbed.

If the corner near the point  $c$  in Fig. 8(a) really does represent an imperfect transcritical bifurcation, then a curve of unstable steady states passes close to it in the manner shown in Fig. 6(b). What would happen if a perturbation carried the system from the corner past the curve of steady states? If the dynamics of the system continues to be described by a single variable, the system must relax to a different, metastable state. If the system relaxes back to the original stable state, it must do so through a mechanism described by more than one state variable. In any case, if a study is made of the response to perturbations near the corner in Fig. 8(a), we predict that there will be a perturbation of critical strength, beyond which the dynamics change.

#### IV. CONCLUSION

We have incorporated the normal form for the unfolded pitchfork bifurcation into a system of stochastic differential equations including both additive and linear noise. The source of the linear noise is modeled by an Ornstein-Uhlenbeck process with finite correlation time  $\gamma^{-1}$ . A formula for the variance of the resultant fluctuations may be readily obtained. We consider this variance as a function of the distinguished parameter  $\lambda$  in the normal form for the pitchfork; this function depends on the relative magnitude of the noise correlation time  $\gamma^{-1}$  and the deterministic relaxation time  $p_s'(\lambda)$ .

For the case of white noise we have found the bifurcation set for extrema in the variance diagram. With hysteresislike imperfections, only one extremum is possible. For transcriticallike imperfections, either one or two extrema may be found. We have also investigated the change in the bifurcation set when the linear noise acquires a finite correlation time. The finite correlation time adds an additional extremum to the variance diagram for transcriticallike imperfections, but does not change the number of extrema in the case of hysteresislike imperfections.

We find good qualitative agreement between the results of Refs. 6 and 7 and our very simple model of the superfluid turbulence transition region near the point  $c$ . The model provides a unified explanation for the parametric behavior of steady states, the characteristic time of relaxation to those steady states, and the power in fluctuations about the steady states. It predicts that, close to the point  $c$ , the response of the system to perturbations whose strength exceeds some critical value will change in a qualitative way.

Our analysis also has several limitations which point in directions toward which this work should be extended. We only investigate the linearized system (4). At a singularity linear terms in the Taylor expansion about the steady state vanish; therefore, our results do not hold too close to a singular point. However, because the bifurcation is imperfect, no singular point is encountered experimentally and our analysis is applicable to the experimental data as demonstrated by the good qualitative agreement. Another consequence of linearization is that our analysis only covers the case of weak noise; again that seems to be the regime for the experiment in Refs. 6 and 7. However, if in different experimental setups a larger amplitude of fluctuations is encountered, higher-order terms in the expansion of the restoring force about the steady state will become important and would have to be retained in the analysis. Finally, we do not take into account the spatial extent of the narrow tube through which the helium flows. Temporal fluctuations at one end of the system may be carried by the flow and therefore become spatial fluctuations. The measured state variable, the free-energy difference between the ends of the tube, must represent some average of local fluctuations. Again, the good qualitative agreement between our theoretical description and the experimental observations suggests that these spatial fluctuations do not strongly affect the dynamics of the measured state variables.

#### ACKNOWLEDGMENTS

We thank J. T. Tough and D. Griswold for stimulating discussions and for making their data available before publication. We also had fruitful discussions with F. Moss and D. Sigeti on aspects of modeling the T-I-T-II transition. One of us (M.F.S.) acknowledges partial support from the Robert A. Welch Foundation (Houston, TX).

- <sup>1</sup>M. Golubitsky and D. G. Schaeffer, *Singularities and Groups in Bifurcation Theory* (Springer-Verlag, New York, 1985).
- <sup>2</sup>(a) J. Ringland, Ph.D. thesis, University of Texas at Austin, Texas, 1986; (b) A. Arneodo, P. H. Couillet, E. A. Spiegel, and C. Tresser, *Physica* **14D**, 327 (1985).
- <sup>3</sup>K. Wiesenfeld, *J. Stat Phys.* **38**, 1070 (1985).
- <sup>4</sup>L. D. Landau, E. M. Lifshitz, and L. P. Pitaevskii, *Statistical Physics, Part I* (Pergamon, Oxford, 1980).
- <sup>5</sup>H. Haken, *Synergetics* (Springer-Verlag, Berlin, 1983).
- <sup>6</sup>C. P. Lorenson, D. Griswold, V. U. Nayak, and J. T. Tough, *Phys. Rev. Lett.* **55**, 1494 (1985).
- <sup>7</sup>D. Griswold, C. P. Lorenson, and J. T. Tough, *Phys. Rev. B* **35**, 3149 (1987).
- <sup>8</sup>(a) J. T. Tough, in *Progress in Low Temperature Physics*, edited by D. F. Brewer (North-Holland, Amsterdam, 1982), Vol. 8, p. 134; (b) R. J. Donnelly and C. E. Swanson, *J. Fluid Mech.* **173**, 387 (1986).
- <sup>9</sup>H. Hoch, L. Busse, and F. Moss, *Phys. Rev. Lett.* **34**, 384 (1975).
- <sup>10</sup>J. A. Northby, *Phys. Rev. B* **18**, 3214 (1978).
- <sup>11</sup>F. Moss and G. V. Welland, *Phys. Rev. A* **25**, 3389 (1982).
- <sup>12</sup>K. W. Schwarz, *Phys. Rev. B* **18**, 245 (1978); K. W. Schwarz, *Phys. Rev. Lett.* **49**, 283 (1982).
- <sup>13</sup>(a) G. Blankenship, G. C. Papanicolaou, *SIAM J. Appl. Math.* **34**, 437 (1978); (b) W. Horsthemke and R. Lefever, *Noise-Induced Transitions* (Springer-Verlag, Berlin, 1984).
- <sup>14</sup>C. W. Gardiner, *Handbook of Stochastic Processes* (Springer-Verlag, Berlin, 1983).